

102-nm-wide, High-gain, Low-noise Lumped Raman Amplifier

Sijing Liang⁽¹⁾, Saurabh Jain⁽¹⁾, Natsupa Taengnoi⁽¹⁾, Kyle R. H. Bottrill⁽¹⁾, Massimiliano Guasoni⁽¹⁾, Yongmin Jung⁽¹⁾, Mengben Xiao⁽²⁾, Periklis Petropoulos⁽¹⁾, David J. Richardson⁽¹⁾, Lin Xu⁽¹⁾

⁽¹⁾ Optoelectronics Research Centre, University of Southampton, Southampton, SO17 1BJ, UK, s.liang@soton.ac.uk

⁽²⁾ HiSilicon Optoelectronics Co., Ltd., Wuhan, Hubei, China

Abstract We present a compact dual-stage lumped Raman amplifier based on 2x1 km lengths of highly nonlinear fibre (HNLF). The amplifier provides 28.5-dB net gain with 4.5-dB optical noise figure (NF) over a bandwidth of 102 nm from 1525 to 1627 nm. ©2023 The Author(s)

Introduction

Lumped Raman amplifiers (LRAs) capable of broadband operation at low-loss telecom wavelengths show great potential for multiband transmission by fully exploiting the transmission window of the existing single-mode fibre network infrastructure to address the immediate demand for increasing data capacity [1-3]. By using a split-combine approach, a multi-stage LRA has recently been demonstrated enabling a 210-nm amplification bandwidth covering the E, S, C and L bands [3]. However, this amplifier provides relatively low gain (15 dB) and a large NF variation ranging between 4.5 and 8.1 dB. In addition, guard-band protection is usually required in such LRAs with >13-THz bandwidth to avoid overlap between signals and the Raman pumps, which precludes seamless broadband operation and reduces the usable bandwidth of an individual LRA. Moreover, broadband Raman amplifiers are prone to suffer from thermal noise generation when used for short-wavelength signals that lie within close-proximity to the longest pump wavelength and which ordinarily results in a large NF tilt across the amplifier bandwidth [4]. The NF tilt in broadband LRAs can be improved by using shorter-wavelength Raman pumps in the co-pumping direction [5], or by distributing the pump wavelengths across two amplifier stages to reduce the thermal noise [6]. However, co-pumping requires a pump laser of low relative intensity noise (RIN) and the dual-stage distributed pumping architecture places a limitation on the total achievable gain. Recently,

we reported an 80-nm-wide dual-stage LRA providing 27-dB flat gain and 5.8-dB NF (<1-dB NF tilt) [7] in which a spectral-gain-control (SGC) method was proposed and shown to be effective in managing the spectral gain profile and the associated thermal noise in each amplifier stage.

In this paper, we show that the ‘SGC’ approach allows extension of the operating bandwidth of a compact dual-stage LRA up to 102 nm (~13 THz) whilst maintaining high-performance amplification. We achieved an average net gain of 28.5 dB with 2.6-dB flatness from 1525 to 1627 nm. The optical NF of the LRA was measured to be 4.5 dB on average with a small variation of 1.2 dB across the full signal wavelength range. The impact of double Rayleigh backscattering (DRS) in our LRA is also discussed in this paper.

Experimental setup

Fig. 1(a) shows a schematic of the experimental setup. The LRA was designed as a dual-stage structure and allowed for active control of the spectral gain in each amplifier stage. Both the first-stage (RA1) and the second-stage (RA2) Raman amplifiers employed 1-km lengths of HNLF such that the total device length was just 2 km. The HNLF (Sumitomo Electric Industries, Ltd.) had a mode field diameter of 3.5 μm , fibre attenuation of 0.6 dB/km at 1550 nm and a peak Raman gain coefficient of 6.9 $\text{W}^{-1}\text{km}^{-1}$ as measured with a 1430-nm pump beam. The Raman pump wavelengths were then determined by simulation based on the Raman gain spectrum

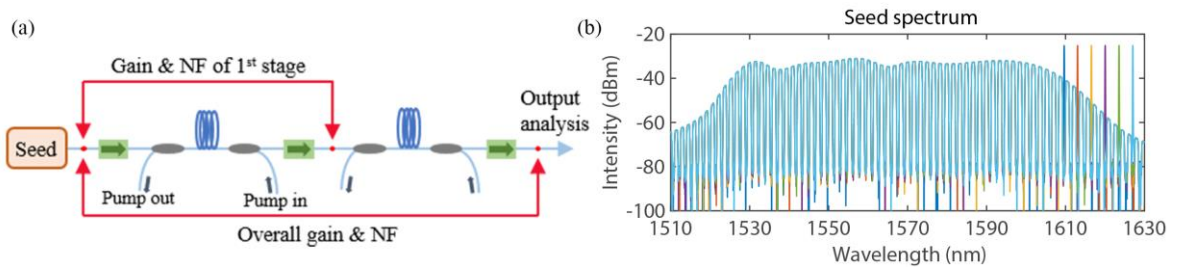


Fig. 1: (a) Schematic of the experimental setup; (b) spectrum of the seed source.

of the HNLF and the target gain bandwidth of 1525-1627 nm. Pump wavelengths of 1426, 1442, 1461, 1485 and 1514 nm were chosen to realize a flat gain profile for this broad wavelength range. Note that in this demonstration we used commercial high-power laser diodes (LDs) for the 14xx-nm pumps and an in-house built erbium doped fibre laser at 1514 nm (FL-1514) due to the lack of off-the-shelf LDs at this particular wavelength. The FL-1514 pump could ultimately be replaced by customised LDs to further improve the system compactness. The HNLFs were counter-pumped to minimize the RIN transfer from pump to signal [8]. Isolators were inserted at the input, output and between the two amplifier stages of the LRA to prevent feedback from unwanted reflections and stop the potential DRS of signals from RA2 going back into RA1. The LRA was characterised by an in-house built broadband seed source which consisted of a multi-channel spectrally-filtered ASE source with 6-dB spectral intensity variation from 1525 to 1605 nm and a single-channel tunable laser source covering the 1606-1627 nm range. Fig. 1(b) shows the spectrum of this integrated seed source. The total power of the seed source was set to -8.2 dBm and launched into the LRA (corresponding to an average input power per channel of -25.3 dBm). The LRA output was characterised by an optical spectrum analyser (OSA) and a power meter.

Results and discussion

Since the overall NF was determined primarily by the NF of RA1, the performance of RA1 was first optimised by controlling the pump power of 1514 nm to tailor the wavelength dependent gain distribution and manage the build-up of thermal noise in RA1. Fig. 2 illustrates how the measured net gain and NF of RA1 evolved with the 1514-nm pump power when the coupled pump powers of 1426, 1442, 1461 and 1485 nm were kept at 672, 190, 179 and 143 mW respectively. As shown by the blue line in Fig. 2, a flat gain profile (~13 dB) from 1525 to 1627 nm was obtained

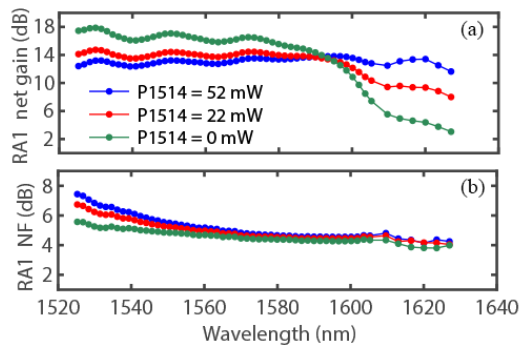


Fig. 2: Measured (a) net gain and (b) NF of RA1 when the coupled pump power of 1514 nm was 52, 22 and 0 mW.

when the 1514-nm pump power was 52 mW. However, the measured NF showed a large tilt (3.2 dB) across the full signal bandwidth with the largest NF of 7.4 dB at 1525 nm. This observation, as expected, was due to the strong thermal noise generation at shorter wavelengths (~1525 nm) arising from noise from the 1514-nm pump being spectrally close to the short signal wavelengths. As the 1514-nm pump power decreased to 22 mW (red line in Fig. 2), the thermal noise generated by the 1514-nm pump and the pump-to-pump energy transfer via the Raman effect were reduced, which subsequently led to a sloped gain profile and improved NF in RA1. The highest NF was reduced to 6.7 dB and the NF tilt was reduced to 2.6 dB. However, it was observed experimentally that the NF at shorter signal wavelengths was degraded even for just a few mW of pump power at 1514 nm launched into the HNLF. This is because the 1514-nm pump can be efficiently amplified in the HNLF by the 1426-nm pump, stealing the gain from the short-wavelength signals and generating thermal noise. When there was no 1514-nm pump in RA1 (green line in Fig. 2), the NF tilt was minimized to 1.8 dB and the maximum NF was only 5.6 dB, due to the much smaller thermal noise contribution from the 1485-nm pump compared to the 1514-nm pump.

Based on these observations, we chose to remove the FL-1514 pump from RA1 in order to achieve a low overall NF (≤ 6 dB) and a small NF tilt (< 2 dB). Accordingly, this required a much higher 1514-nm pump power in RA2 to provide for gain compensation at longer wavelengths (~1600-1627 nm). The FL-1514 pump for RA2 was operated at 329 mW to demonstrate the high and flat gain operation of the LRA. Note that the coupled pump powers of 1426, 1442, 1461 and 1485 nm in RA1 and RA2, summarised in Tab.1, were carefully optimised to achieve high overall gain with < 3 -dB gain flatness. The measured gain profiles are plotted in Fig. 3(a) and compared with our simulation. The two amplifier stages showed different sloped gain profiles which are complementary to each other, resulting in an average overall gain of 28.5 dB with 2.6-dB gain variation from 1525 to 1627 nm. The experimental results are in good agreement with the simulations, as seen in Fig. 3(a). The highest

Tab. 1: Coupled pump powers used in the LRA.

Pump	1 st stage (mW)	2 nd stage (mW)
LD-1426	839	789
LD-1442	151	277
LD-1461	194	253
LD-1485	122	74
FL-1514	0	329

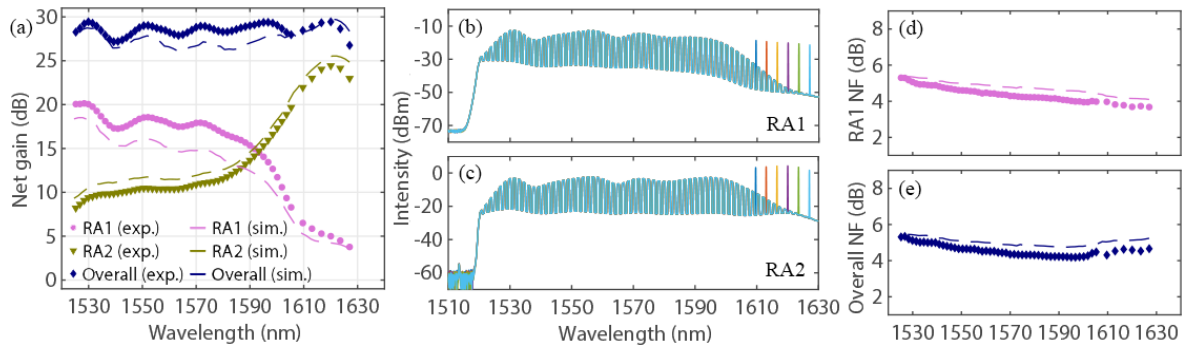


Fig. 3: (a) Measured and calculated gain profiles of the LRA; output spectra of (b) RA1 and (c) RA2; (d) measured and calculated NF of RA1; (e) measured and calculated overall NF.

net gain in RA1 was measured to be 20.1 dB at 1528 nm whereas the maximum net gain in RA2 was 24.4 dB at 1620 nm.

The output spectra of RA1 and RA2 are shown in Fig.3(b) and (c). An output OSNR of >20 dB was recorded for most signal channels at a resolution of 0.2 nm. Fig.3(d) and (e) illustrate the noise performance of the LRA. The NF was experimentally characterised using the standard optical method with the OSA resolution set to 0.2 nm. As shown in Fig. 3(d), the NF of RA1 decreased with signal wavelength from 5.3 dB at 1525 nm to 3.7 dB at 1627 nm. The NF tilt was 1.6 dB after amplification in RA1. The change of NF, in Fig. 3(e), was negligible for signal wavelengths of <1590 nm after second-stage amplification, whereas a small degradation in NF was observed at the longer signal wavelengths (>1590 nm) due to the large gain and increased ASE in RA2. As a result, the overall NF was between 4.2 and 5.4 dB (4.5 dB on average) with a small variation of 1.2 dB. The measured NF matched well with our simulations. Note that the DRS effect and its associated contribution to the NF were considered in our simulation by including the measured Rayleigh coefficient (0.0013 km^{-1}) of the HNLF. Also note that the optical NF measurement is unable to resolve low-frequency noise (e.g., DRS and pump-to-signal RIN transfer), which can lead to an underestimation of the NF. In Fig. 4, we show the calculated overall NF comparison when DRS is considered or not. It can be seen that DRS induces more noise to the signals when the single-stage net gain is higher (i.e., signals

around 1530 nm in RA1 and signals around 1620 nm in RA2). Despite high single-stage gain at these particular wavelengths, the DRS-induced noise in our LRA was relatively small and only degraded the overall NF by ~ 0.1 dB, thanks to the inter-stage isolation and the short length of HNLF used in each stage. Another source of noise, which was not considered in our simulation and also not resolvable by the OSA, is pump-to-signal RIN transfer. An electrical NF measurement is favoured for further analysing the noise performance of the LRA and will be performed in due course.

Conclusion

We have demonstrated a 102-nm-wide, high-gain, low-noise lumped Raman amplifier enabled by employing 2x1 km lengths of HNLF in a dual-stage structure and manipulating the wavelength dependent gain distributions in the two amplifier stages. Our results further highlight the potential of high-performance wideband lumped Raman amplifiers for providing upgrades to the existing single-mode fibre networks to expand data capacity for massive communication applications in the near future.

References

- [1] M. A. Iqbal, M. Tan, W. Forsyiaak and A. Lord, "Opportunities and Challenges for Discrete Raman Amplifiers in Ultrawideband Transmission Systems," in *IEEE Photonics Society Summer Topicals Meeting Series (SUM)*, Cabo San Lucas, Mexico, 2022, pp. 1-2, DOI: [10.1109/SUM53465.2022.9858323](https://doi.org/10.1109/SUM53465.2022.9858323)
- [2] P. Hazarika, M. Tan, A. Donodin, S. Noor, I. Phillips, P. Harper, J. S. Stone, M. J. Li, and W. Forsyiaak, "E-, S-, C- and L-band coherent transmission with a multistage discrete Raman amplifier," *Optics Express*, vol. 30, no. 24, pp. 43118-43126, 2022, DOI: [10.1364/OE.474327](https://doi.org/10.1364/OE.474327)
- [3] P. Hazarika, M. Tan, A. Donodin, I. Phillips, P. Harper, M. Li, and W. Forsyiaak, "210 nm E, S, C and L Band Multistage Discrete Raman Amplifier," in *Optical Fiber Communication Conference (OFC)*, San Diego, USA, 2022, paper Tu3E.2, DOI: [10.1364/OFC.2022.Tu3E.2](https://doi.org/10.1364/OFC.2022.Tu3E.2)
- [4] M. N. Islam, "Raman amplifiers for telecommunications," *IEEE Journal of Selected Topics in Quantum Electronics*,

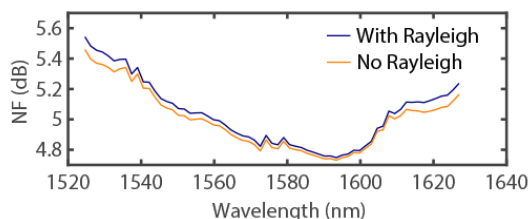


Fig. 4: Calculated overall NF with and without consideration of DRS-induced noise.

vol. 8, no. 3, pp. 548-559, 2002, DOI:
[10.1109/JSTQE.2002.1016358](https://doi.org/10.1109/JSTQE.2002.1016358)

- [5] S. Kado, Y. Emori, S. Namiki, N. Tsukiji, J. Yoshida and T. Kimura, "Broadband flat-noise Raman amplifier using low-noise bidirectionally pumping sources," in *Proceedings 27th European Conference on Optical Communication*, Amsterdam, Netherlands, 2001, pp. 38-39 vol.6, DOI: [10.1109/ECOC.2001.989038](https://doi.org/10.1109/ECOC.2001.989038)
- [6] M. A. Iqbal, Ł. Krzczanowicz, I. D. Philips, P. Harper and W. Forsyia, "Noise Performance Improvement of Broadband Discrete Raman Amplifiers Using Dual Stage Distributed Pumping Architecture," *Journal of Lightwave Technology*, vol. 37, no. 14, pp. 3665-3671, 2019, DOI: [10.1109/JLT.2019.2919383](https://doi.org/10.1109/JLT.2019.2919383)
- [7] S. Liang, S. Jain, L. Xu, K. R. H. Bottrill, N. Taengnoi, M. Guasoni, P. Zhang, M. Xiao, Q. Kang, Y. Jung, P. Petropoulos, and D. J. Richardson, "High Gain, Low Noise, Spectral-Gain-Controlled, Broadband Lumped Fiber Raman Amplifier," *Journal of Lightwave Technology*, vol. 39, no. 5, pp. 1458-1463, 2021, DOI: [10.1109/JLT.2020.3034678](https://doi.org/10.1109/JLT.2020.3034678)
- [8] C. R. S. Fludger, V. Handerek and R. J. Mears, "Pump to signal RIN transfer in Raman fiber amplifiers," *Journal of Lightwave Technology*, vol. 19, no. 8, pp. 1140-1148, 2001, DOI: [10.1109/50.939794](https://doi.org/10.1109/50.939794)